Journal of Integrative Neuroscience

J. Integr. Neurosci. **2026**; 25(11): 52110
https://doi.org/10.31083/JIN52110

Original Research

Estrogen Modulates the Bidirectional Interplay Between Microglial Inflammation and the Tryptophan-Kynurenine Pathway in Ovariectomy-Induced Depression

Hao Zhang[1], Yangzhi Xie[1], Yili Yi[1], Can Wang[1], Zhengyang Yuan[1], Fan Xiao[2,*], Li Jiang[1,*]

[1]Department of Neurology, The Affiliated Nanhua Hospital, Hengyang Medical School, University of South China, 421002 Hengyang, Hunan, China
[2]Clinical Research Institute, The Affiliated Nanhua Hospital, Hengyang Medical School, University of South China, 421002 Hengyang, Hunan, China
*Correspondence: xiaof-usc@foxmail.com (Fan Xiao); jiangli_usc@126.com (Li Jiang)

Academic Editors: Ashutosh Tripathi and Bettina Platt
Submitted: 20 March 2026 Revised: 28 June 2026 Accepted: 20 July 2026 Published: 10 November 2026

Abstract

Background: The neurobiological mechanisms connecting the increased susceptibility to depression to postmenopausal estrogen depletion remain incompletely understood. In this study, we examined the hypothesis that ovariectomy (OVX)-induced depression-like behaviors are associated with dysregulation of microglial activation and the disruption of the tryptophan (Trp)-kynurenine (Kyn) metabolic pathway. We also evaluated whether 17β-estradiol (E2) can reestablish homeostasis within these interconnected systems. **Methods:** Adult female C57BL/6 mice were randomly assigned to one of four groups: sham-operated control (Control), OVX, OVX+low-dose E2 (Low), and OVX+high-dose E2 (High). Depression-like behaviors were assessed using standardized tests, including the sucrose preference test, forced swimming test, open field test, and tail suspension test. Hippocampal integrity was evaluated using Nissl staining and quantitative histomorphometry. Transcriptomic profiling was performed on *ex vivo*-isolated primary microglia obtained from the Control and OVX groups. Subsequent analyses included quantification of inflammatory cytokines using enzyme-linked immunosorbent assay (ELISA); assessment of microglial M1 polarization by immunofluorescence staining for inducible nitric oxide synthase (iNOS) and ionized calcium-binding adapter molecule 1 (Iba1); assessment of nuclear levels of phosphorylated nuclear factor kappa-light-chain-enhancer of activated B cells (NF-κB) p65 (Ser468) using Western blot; determination of hippocampal microglial levels of Trp, Kyn, and serotonin (5-HT) using ELISA; and analysis of the key proteins involved in tryptophan and serotonin metabolism, including tryptophan hydroxylase 2 (TPH2), serotonin transporter (SERT), monoamine oxidase A (MAO-A), and indoleamine 2,3-dioxygenase 1 (IDO1) using Western blot. **Results:** OVX mice exhibited significant depression-like behaviors and hippocampal neuronal loss, both of which were mitigated by E2 supplementation in a dose-dependent manner. Transcriptomic analysis revealed pronounced enrichment of NF-κB signaling and related inflammatory pathways in microglia from OVX mice. Consistent with these findings, the OVX group showed elevated levels of tumor necrosis factor-alpha (TNF-α), interleukin-1 beta (IL-1β), and interleukin-6 (IL-6) in hippocampal microglia, an increased proportion of iNOS-positive M1-polarized microglia, increased nuclear phospho-NF-κB p65 (Ser468) abundance, decreased levels of hippocampal microglial Trp and 5-HT, elevated Kyn, reduced expression of TPH2 and SERT, and upregulated expression of IDO1 and MAO-A. **Conclusions:** These results suggest that estrogen deficiency is associated with a coordinated set of changes, including depressive behavior, microglia-associated neuroinflammation, and a metabolic shift in Trp catabolism toward the Kyn pathway. E2 administration restored these parameters, highlighting an integrated view of neuroimmune and metabolic alterations in a model of post-ovariectomy depression.

Keywords: depression; estrogen; neuroinflammation; microglia

1. Introduction

Depression is a leading cause of disability worldwide, and women have a significantly higher incidence of depression during perimenopause [1]. Perimenopause is characterized by a significant decline in endogenous estrogen levels, which is closely linked to the emergence of depressive symptoms. Clinical observations support the therapeutic potential of estrogen to alleviate these symptoms, but its use remains limited due to unresolved risks and differences in efficacy [2,3]. A key obstacle to optimizing treatment is the incomplete understanding of the specific neural mechanisms through which estrogen deficiency increases susceptibility to depression. Therefore, clarifying these mechanisms is crucial for developing safer and more precise neuroendocrine-based intervention strategies.

An increasing body of evidence indicates that neuroinflammation is a key mediator in stress-related mental disorders [4,5]. In the brain, microglia serve as the primary immune sentinels. Estrogen has well-recognized anti-inflammatory effects, and its deficiency may prompt microglia to shift toward a pro-inflammatory state [6]. This activated phenotype involves the release of cytokines, such as interleukin-1 beta (IL-1β) and tumor necrosis factor-alpha (TNF-α), which are typically regulated by the nu-

Copyright: © 2026 The Author(s). Published by IMR Press.
This is an open access article under the CC BY 4.0 license.

Publisher's Note: IMR Press stays neutral with regard to jurisdictional claims in published maps and institutional affiliations.

clear factor kappa-light-chain-enhancer of activated B cells (NF-κB) signaling pathway [7]. These inflammatory signals may disrupt synaptic plasticity and neuronal function, providing a plausible physiological basis for depressive behavior [8,9]. Notably, this pathway represents a specific target for clinical intervention, linking systemic hormonal changes to brain pathophysiology.

Inflammation profoundly affects brain metabolism, particularly the metabolic fate of the essential amino acid tryptophan (Trp) [10,11]. Under inflammatory conditions, the indoleamine 2,3-dioxygenase 1 (IDO1) enzyme is induced and activated, diverting Trp metabolism away from the pathway that synthesizes serotonin (5-HT), a key monoamine involved in mood regulation, toward the kynurenine (Kyn) pathway [12,13]. This shift not only reduces the availability of 5-HT but may also increase the production of neuroactive Kyn metabolites with potential neurotoxic effects. Thus, inflammation-driven Trp metabolic dysregulation establishes a direct metabolic link between immune activation and the neurochemical alterations observed in depression. Based on these observations, an integrative hypothesis has emerged: the clinical phenomenon of postmenopausal depression may partly result from a coordinated sequence in which estrogen deficiency prompts microglial activation and NF-κB-mediated neuroinflammation; this inflammatory environment then upregulates IDO1, shifting Trp metabolism from 5-HT production toward the Kyn pathway. The combined effect of intensified inflammation and a monoamine/precursor metabolic disorder may jointly drive the depressive pathological process. However, direct experimental evidence confirming the mechanism of this multi-system interaction in estrogen-deficiency models is currently lacking.

To fill this gap and provide a reference for translational medical research, a preclinical model of surgical menopause was established through ovariectomy (OVX). It was hypothesized that OVX-induced depressive-like behaviors would be associated with two factors: the parallel exacerbation of microglia-driven neuroinflammation and the shift of hippocampal Trp metabolism towards pathogenicity. Additionally, it was speculated that estrogen replacement therapy with 17β-estradiol (E2) would restore these indicators to normal. This study integrated behavioral analysis, histological assessment, microglial transcriptomics, and the evaluation of inflammatory and metabolic pathways. It aimed to depict an interrelated neuroimmune-metabolic mechanism, thereby clarifying the underlying pathophysiological processes in estrogen deficiency and highlighting potential targets for future therapeutic research.

2. Methods

2.1 Animals and Ethics

Adult female C57BL/6 mice (10–12 weeks of age) were obtained from Gempharmatech (Nanjing, Jiangsu, China). The animals were group-housed (4–5 per cage) under controlled environmental conditions, including a 12-h light/dark cycle (lights on at 7:00 AM), a constant ambient temperature (22 ± 1 °C), and 40–60% relative humidity. Standard rodent chow and tap water were available *ad libitum.* All mice were acclimatized to the housing facility for at least 1 week before any experimental procedures.

2.2 Experimental Groups and Surgical Procedure

Following acclimatization, mice were randomly assigned to one of four experimental groups: (1) Sham-operated control (Control), (2) the OVX group, (3) OVX with low-dose E2 replacement (OVX+Low E2), and (4) OVX with high-dose E2 replacement (OVX+High E2). Bilateral ovariectomy was performed under isoflurane anesthesia (3–4% for induction and 1.5–2% for maintenance; MedChemExpress, Monmouth Junction, NJ, USA; Cat. No. HY-A0134), following a previously described procedure [14] with minor modifications. A dorsal midline incision was made, the ovarian bursa was identified, and the ovaries were excised after ligation of the oviduct. The muscle layer and skin were then sutured. Sham-operated mice underwent an identical procedure in which the ovaries were exteriorized but not removed. Postoperative analgesia was provided via subcutaneous injection of carprofen (HY-B1227, MedChemExpress) (5 mg/kg) for 48 h. Mice were monitored daily for signs of pain or distress during a standard four-week postoperative recovery period to establish a stable hypoestrogenic state.

2.3 Estradiol Treatment Regimen

E2 replacement therapy began four weeks after surgery. E2 (Sigma-Aldrich, St. Louis, MO, USA, E8875) was dissolved in a sterile corn oil (HY-Y1888, MedChemExpress) vehicle. Mice in the OVX+Low E2 and OVX+High E2 groups received daily subcutaneous injections of E2 at doses of 1.0 µg/mouse/day and 5.0 µg/mouse/day, respectively, for four consecutive weeks. Control and OVX groups received daily injections of an equivalent volume of corn oil vehicle. The efficacy of the OVX procedure and E2 replacement was biochemically validated at the study endpoint by quantifying serum E2 levels using a commercially available mouse E2 enzyme-linked immunosorbent assay (ELISA) kit (Mouse Estradiol ELISA Kit, Abcam, Cambridge, UK, ab108667). Dose selection was based on preliminary experiments and prior literature [14]: the low dose (1.0 µg/mouse/day) was chosen to bring serum estradiol levels into the physiological range of intact female mice, mimicking low-dose estrogen replacement therapy in perimenopausal women; the high dose (5.0 µg/mouse/day) was selected to produce supraphysiological levels, corresponding to the upper range of clinical hormone replacement therapy. These two doses allow us to explore physiological replacement and potential dose-dependent effects, aiding translational links to human studies with different dosing regimens.

2.4 Behavioral Phenotyping

Depression-like behaviors were assessed through a series of standardized tests during the final experimental phase. All behavioral evaluations were performed during the light cycle by an investigator blinded to group allocation, with at least 48 h between successive tests.

The sucrose preference test was conducted to evaluate anhedonia [15]. Mice were acclimated for over 24 h to two bottles containing a 1% sucrose solution. Following a 24-h water deprivation period, each animal was given free access to one bottle of 1% sucrose solution and one bottle of plain water for a 12 h test period. To control for side preference, bottle positions were alternated at the 6-h mark. Sucrose preference was determined by calculating the percentage of sucrose consumption relative to total fluid intake.

The tail suspension test was employed to measure behavioral despair [16]. After an adaptation period, each mouse was suspended by the tail 30 cm above the floor for a total of 6 min. Immobility duration was recorded during the final 4 min of the test.

The forced swimming test was performed to assess depressive-like immobility further [17]. Mice were acclimated to swimming one day before testing. Twenty-four h later, each animal was placed in a transparent cylinder (25 cm in height, 15 cm in diameter) filled with water (23–25 °C) and monitored for 5 min. Immobility time was recorded throughout the 5-min session.

The open field test was performed to assess exploratory activity [18]. After a period of acclimation to the testing room, each mouse was placed in a square open-field arena (1 × 1 m) and allowed to explore freely for 4 min. Rearing frequency, defined as the number of times the animal stood upright on its hind legs, was manually recorded throughout the entire 4 min observation period.

Twenty-four h after the final behavioral test, mice were administered an overdose of sodium pentobarbital (150 mg/kg, P3761, Sigma-Aldrich). Blood samples were obtained via cardiac puncture for serum separation. The brain was swiftly extracted and hemisected on an ice-cold dissection platform. The left hemisphere was immersion-fixed in 4% paraformaldehyde (P6148, Sigma-Aldrich) in 0.1 M phosphate buffer (pH 7.4) for 48 h at 4 °C to enable subsequent histological analysis. The right-hemisphere hippocampus was micro-dissected, flash-frozen in liquid nitrogen, and stored at –80 °C for molecular analysis.

2.5 Histological and Morphometric Analysis

Both hematoxylin and eosin (H&E) and Nissl staining were performed on paraffin-embedded coronal brain sections to assess neuronal integrity in the hippocampal Cornu Ammonis area 3 (CA3) subfield. For H&E staining, sections were dewaxed, stained, examined, and imaged using a light microscope (Nikon 90i, Nikon, Tokyo, Japan). Pyknotic nuclei in the CA3 region were quantified. For Nissl staining, sections were stained with cresyl violet (C5042, Sigma-Aldrich), and damaged neurons in the CA3 region were counted. All histological analyses were blinded.

2.6 Primary Microglial Isolation and Transcriptomic Profiling

Primary microglia were isolated from the hippocampi of separate cohorts of Control and OVX mice that were not subjected to behavioral testing, using a protocol adapted from previous reports [19,20] with modifications. Briefly, mice were deeply anesthetized with sodium pentobarbital (50 mg/kg, i.p.) and transcardially perfused with ice-cold phosphate-buffered saline (PBS) to remove blood cells. The hippocampi were rapidly dissected and minced with sterile scalpel blades. The minced tissue was enzymatically dissociated in Hanks' Balanced Salt Solution (HBSS; Gibco, Grand Island, NY, USA, 14175095) containing papain (2 mg/mL; Worthington, Lakewood, NJ, USA, LS003126) and DNase I (0.5 mg/mL; Sigma-Aldrich, D5025) for 30 min at 37 °C with gentle agitation. Digestion was terminated by adding an equal volume of HBSS supplemented with 10% fetal bovine serum (FBS; Gibco, 16000044). The suspension was mechanically triturated using fire-polished Pasteur pipettes with decreasing opening diameters (approximately 1.0 mm, 0.6 mm, and 0.3 mm) to triturate the tissue, then passed through a 70-µm cell strainer (Corning Incorporated, Corning, NY, USA, 352350) to obtain a single-cell suspension. The filtrate was centrifuged at 300 ×g for 10 min at 4 °C, and the pellet was resuspended in 30% Percoll (GE Healthcare, Chicago, IL, USA, 17-0891-01) prepared in PBS. This suspension was carefully layered onto a 70% Percoll cushion in a 15-mL centrifuge tube. Density gradient centrifugation was performed at 900 ×g for 30 min at 4 °C with the brake turned off to maintain gradient integrity. The 30/70% discontinuous gradient was chosen because it effectively separates microglia (which accumulate at the 30/70 interface) from myelin debris and other cell types, providing a balance between yield and enrichment without the need for more complex multi-step gradients. The microglia-enriched interface was collected, washed twice with PBS, and pelleted at 300 ×g for 10 min. No antibody-based purification was performed; therefore, the collected cells represent a microglia-enriched population rather than purified microglia. Cell viability was assessed by trypan blue exclusion and consistently exceeded 90%. Purity was routinely estimated by cytospin preparation followed by immunostaining for ionized calcium-binding adapter molecule 1 (Iba1), which typically showed >80% $Iba1^+$ cells. The isolated cells were validated by morphological assessment and Iba1 immunostaining, and tested negative for mycoplasma contamination. The isolated microglia were used immediately for RNA extraction, ELISA, and Western blot analyses.

Total RNA was extracted using the RNeasy Plus Mini Kit (Qiagen, Hilden, Germany, 74134) according to the manufacturer's instructions. RNA integrity was verified with an Agilent 2100 Bioanalyzer (Agilent Technolo-

gies, Santa Clara, CA, USA, G2939BA) using RNA 6000 Nano chips (5067-1511; Agilent Technologies); all samples had RNA Integrity Number (RIN) >8.0. Stranded mRNA libraries were prepared using the NEBNext Ultra II Directional RNA Library Prep Kit (NEB, Ipswich, MA, USA, E7760L) and sequenced on an Illumina NovaSeq 6000 platform (Illumina, San Diego, CA, USA, 20012850) with paired-end 150 bp reads. Raw reads were quality-controlled with FastQC (v0.11.9, Babraham Bioinformatics, Cambridge, UK), aligned to the mouse reference genome GRCm39 using STAR (v2.7.10a, Cold Spring Harbor Laboratory, Cold Spring Harbor, NY, USA), and gene-level counts were quantified with featureCounts (v2.0.3, WEHI, Melbourne, VIC, Australia). Differential expression analysis was performed with DESeq2 (v1.38.3, Bioconductor, Seattle, WA, USA) in R (v4.2.1, R Foundation for Statistical Computing, Vienna, Austria). Gene Set Enrichment Analysis (GSEA, v4.3.2, Broad Institute, Cambridge, MA, USA) and Kyoto Encyclopedia of Genes and Genomes (KEGG) pathway enrichment were carried out using clusterProfiler (v4.6.0, The University of Hong Kong, Hong Kong, China) to identify significantly altered biological processes.

2.7 Immunofluorescence Staining

To assess microglial morphology and activation status, free-floating coronal brain sections (30 µm thick) were blocked, permeabilized, and then incubated overnight at 4 °C with primary antibodies: rabbit anti-Iba1 (1:500, Wako, Osaka, Japan, 019-19741, RRID: AB_839504) and mouse anti-inducible nitric oxide synthase (iNOS, 1:200, Santa Cruz, Dallas, TX, USA, sc-7271, RRID: AB_2891105). After washing, the sections were incubated with suitable fluorescent secondary antibodies (Alexa Fluor 488 and 594, 1:500, Invitrogen, Carlsbad, CA, USA) for two h at room temperature. Nuclei were counterstained with 4′,6-Diamidino-2-phenylindole (DAPI) (124653, Sigma-Aldrich). Z-stack images were acquired using a laser scanning confocal microscope (Zeiss, LSM 880). For qualitative morphological assessment, $Iba1^+$ cells were categorized into three phenotypes: ramified (small soma with thin, long, highly branched processes), activated (enlarged soma with shorter, thicker processes), and amoeboid (round soma with few or no processes). The number of $Iba1^+$ cells and the proportion exhibiting iNOS co-localization (M1-like phenotype) within the hippocampal formation were quantified.

2.8 Enzyme-Linked Immunosorbent Assay (ELISA)

Primary microglia, isolated as described in section 2.6, were lysed in cold PBS supplemented with a protease inhibitor cocktail. Homogenates were centrifuged, and the supernatant was collected for analysis. Concentrations of pro-inflammatory cytokines (IL-1β, TNF-α, interleukin-6 [IL-6]) and key metabolites of the Trp pathway (Trp, Kyn, 5-HT, 5-Hydroxyindoleacetic acid) were measured utilizing specific, commercially available mouse ELISA kits according to the manufacturer's protocol. All samples were run in duplicate, and absorbance was read on a microplate reader (VLBL00D0, Thermo Fisher Scientific). The ELISA kits used in this part of the experiment are listed as follows: Mouse TNF-α ELISA Kit (R&D Systems, Minneapolis, MN, USA, MTA00B); Mouse IL-1β ELISA Kit (R&D Systems, MLB00C); Mouse IL-6 ELISA Kit (R&D Systems, M6000B). Mouse Trp ELISA kit (Assay Genie, Dublin, Ireland, AEKE03090), Mouse KYN ELISA kit (Assay Genie, MOFI01315), Mouse Serotonin (5-HT) ELISA kit (Cusabio, Wuhan, Hubei, China, CSB-E08365m), and 5-hydroxyindoleacetic acid (5-HIAA) ELISA kit (Shanghai Jianglai Biotechnology Co., Ltd., Shanghai, China, JL54683).

2.9 Western Blot Analysis

Primary microglia pellets were lysed in radioimmunoprecipitation assay (RIPA) lysis buffer (89900, Thermo Fisher Scientific). For the analysis of nuclear phospho-NF-κB p65 (Ser468) abundance, nuclear and cytoplasmic proteins were extracted using a commercial kit (78833, Thermo Fisher Scientific). Protein concentrations were determined by bicinchoninic acid (BCA) assay. Equal amounts of protein (20–40 µg) were separated by sodium dodecyl sulfate–polyacrylamide gel electrophoresis (SDS-PAGE) and transferred to polyvinylidene fluoride (PVDF) membranes (IPVH00010, Millipore). After blocking, membranes were probed overnight at 4 °C with the following primary antibodies: rabbit anti-phospho-NF-κB p65 (Ser468) (1:1000, Cell Signaling Technology, Beverly, MA, USA, 3039S, RRID: AB_330579), rabbit anti-tryptophan hydroxylase 2 (TPH2, 1:1000, Cell Signaling Technology, 51124, RRID: AB_2799385), rabbit anti-serotonin transporter (SERT, 1:1000, Abcam, AB102048), rabbit anti-monoamine oxidase A (MAO-A, 1:1000, Abcam, AB126751), and rabbit anti-IDO1 (1:800, Abcam, AB311847). Rabbit monoclonal anti-glyceraldehyde-3-phosphate dehydrogenase (GAPDH, 1:5000, Abcam, ab181602) and rabbit anti-TATA-binding protein (1:5000, Huabio, Hangzhou, Zhejiang, China, HA500518) were employed as loading controls for cytoplasmic and nuclear fractions, respectively. Membranes were then incubated with horseradish peroxidase (HRP)-conjugated secondary antibodies (Proteintech, SA00001-2; Thermo Fisher Scientific, M32407) and visualized using an enhanced chemiluminescence substrate. Band intensities were quantified using Image Lab software (version: 6.1, Bio-Rad, Hercules, CA, USA) and normalized to their respective loading controls.

2.10 Statistical Analysis

All quantitative data are presented as the mean ± standard error of the mean (SEM). Statistical analyses were performed using SPSS software (Version 22.0, Armonk,

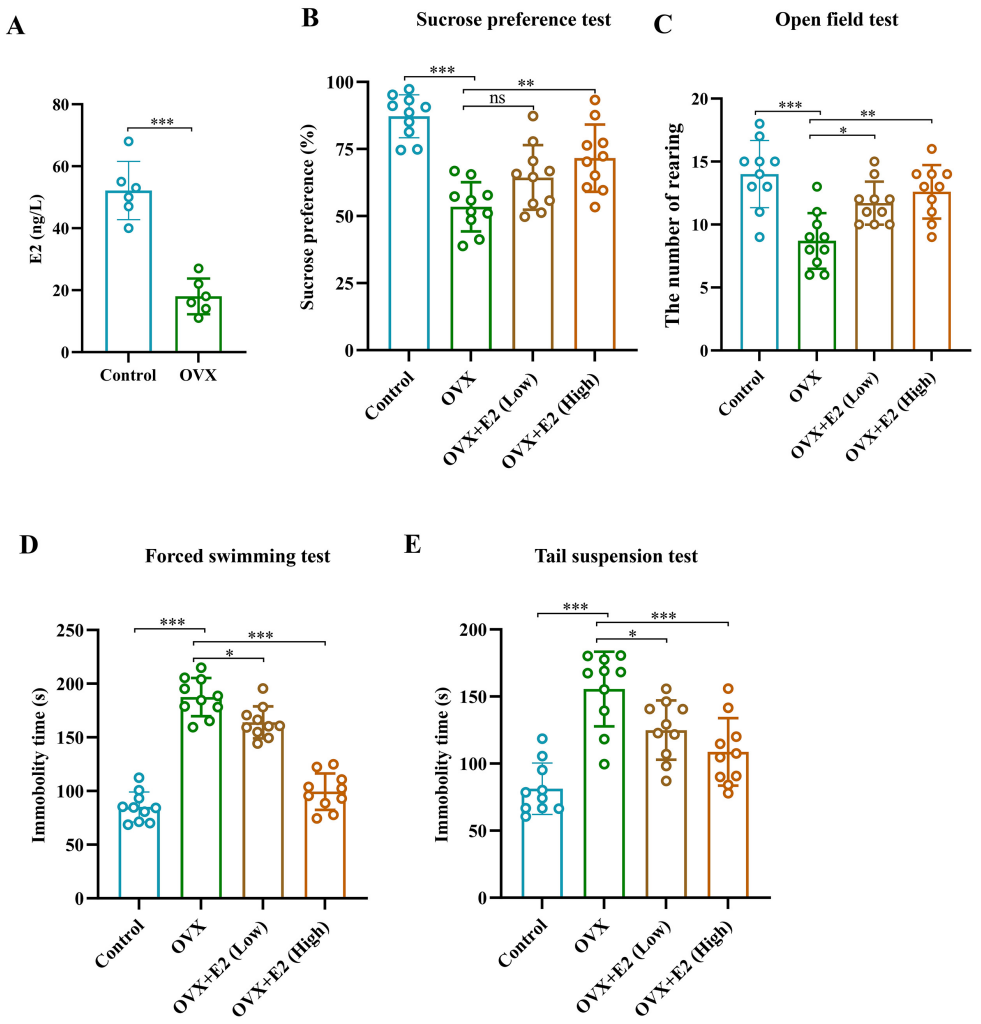


Fig. 1. Effect of OVX and estradiol treatment on depression-like behavior (n = 6 per group for panel A; n = 10 per group for panels B–E). (A) Serum E2 concentrations measured by ELISA. (B) Sucrose preference test. (C) Open field test rearing counts. (D) Immobility time in the forced swimming test. (E) Immobility time in the tail suspension test. ns, not significant, *$p < 0.05$, **$p < 0.01$, ***$p < 0.001$. OVX, ovariectomy; ELISA, enzyme-linked immunosorbent assay; E2, 17β-estradiol.

NY, USA). For comparisons among the four experimental groups, one-way analysis of variance was used, followed by Tukey's *post hoc* test for multiple comparisons. A *p*-value of less than 0.05 was assumed statistically significant for all tests.

3. Results

3.1 Ovariectomy Aggravates and Estradiol Rescues Depressive-Like Phenotypes

Depressive-like behaviors were assessed through a comprehensive battery of tests. OVX significantly decreased circulating estrogen levels (ELISA, $p < 0.001$, Fig. 1A) and induced a depressive phenotype, characterized by reduction in sucrose preference ($p < 0.001$, Fig. 1B), diminished locomotor activity in the open field test ($p < 0.001$, Fig. 1C), and increased immobility time in both the forced swim ($p < 0.001$, Fig. 1D) and the tail suspension tests ($p < 0.001$, Fig. 1E) compared to controls subjects. Notably, E2 treatment in a dose-dependent manner reversed these behavioral impairments. When compared to the OVX group, E2 administration enhanced sucrose preference ($p = 0.003$; Fig. 1B), while the low dose showed no significant change ($p = 0.117$), improved exploratory behavior in the open field (Low: $p = 0.021$; High: $p = 0.002$; Fig. 1C) and reduced immobility duration in the forced swim (Low: $p = 0.011$; High: $p < 0.001$; Fig. 1D) and tail suspension tests (Low: $p = 0.033$; High: $p < 0.001$; Fig. 1E). These findings suggest that OVX is associated with depressive-like behaviors, which are alleviated by E2 in a dose-dependent manner.

3.2 Ovariectomy Aggravates and Estradiol Rescues Hippocampal Pathological Changes

Histopathological alterations in the hippocampus were assessed using H&E (Fig. 2A) and Nissl staining (Fig. 2C). Compared to the Control group, both H&E ($p < 0.001$, Fig. 2B) and Nissl staining ($p < 0.001$, Fig. 2D)

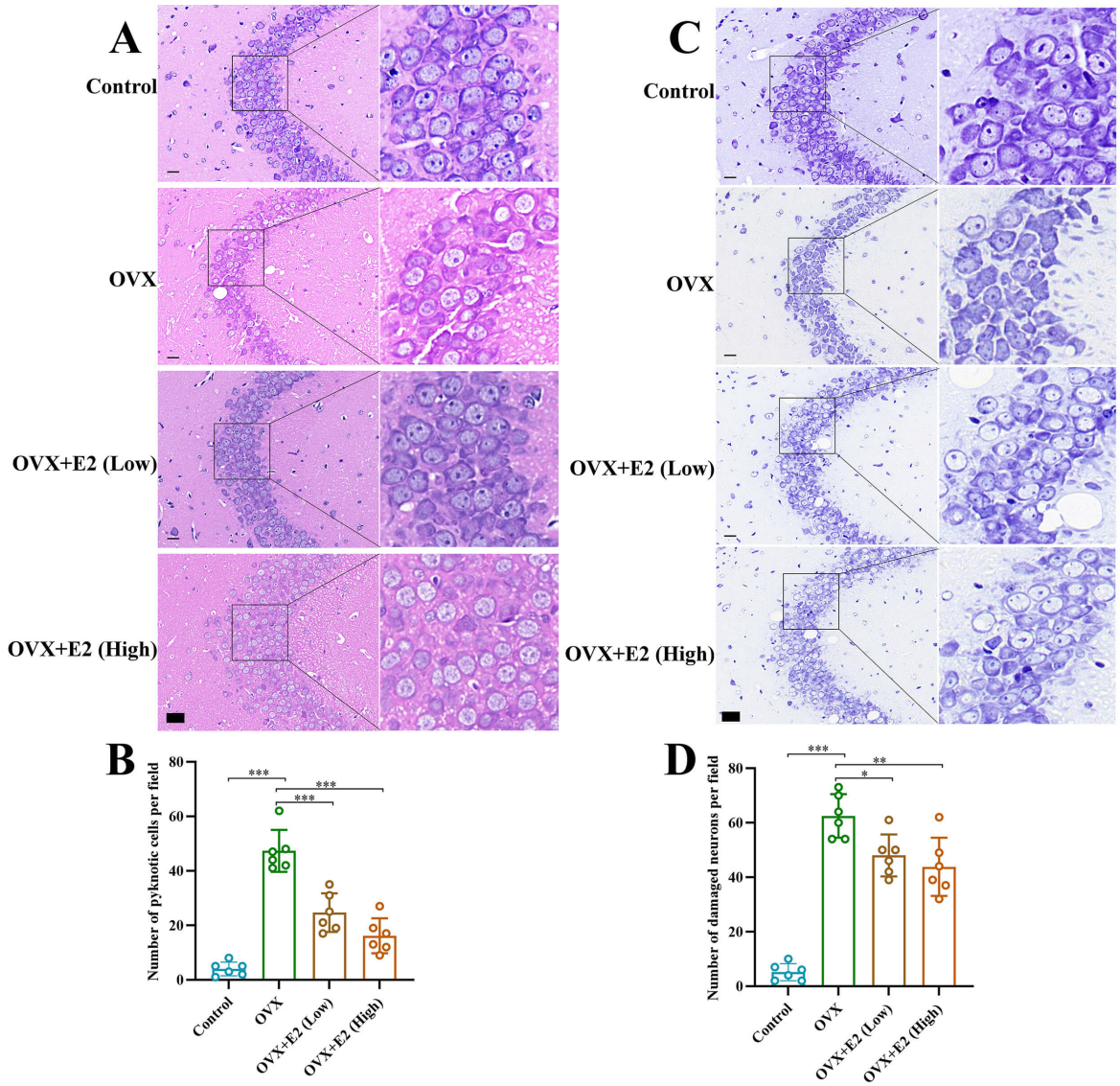


Fig. 2. Effects of OVX and estradiol treatment on Hippocampal pathological changes (n = 6). (A) Representative Hematoxylin and Eosin staining in the CA3 subfield of the hippocampus. (B) Bar graph showing the number of pyknotic cells. (C) Representative Nissl staining in the CA3 subfield of the hippocampus. (D) Bar graph showing the number of damaged neurons. *$p < 0.05$, **$p < 0.01$, ***$p < 0.001$. Scale bar = 20 µm. CA3, Cornu Ammonis area 3.

marked hippocampal damage in the OVX group, characterized by increased pyknotic nuclei and increased numbers of damaged neurons in Nissl-stained sections. Notably, E2 treatment ameliorated these OVX-induced changes in a concentration-dependent manner. Relative to the OVX group, increasing the E2 concentrations progressively attenuated neuronal damage, as evidenced by the significantly decreased numbers of pyknotic nuclei (Low: $p < 0.001$; High: $p < 0.001$; Fig. 2B) and damaged neurons in Nissl-stained sections (Low: $p = 0.018$; High: $p = 0.004$; Fig. 2D). These findings suggest that OVX induces pathological hippocampal alterations, while E2 replacement concentration-dependently ameliorates OVX-mediated hippocampal damage.

3.3 Transcriptional Analysis of Primary Microglia From OVX Mice

To explore the molecular basis underlying the effects of ovariectomy on microglia, we performed transcriptomic profiling of primary microglia isolated from OVX and wild-type (WT) mice. Principal component analysis revealed a clear separation between the two groups (Fig. 3A), indicating that OVX induced a distinct transcriptional reprogramming. The heatmap further demonstrated widespread alterations in gene expression, with large clusters of genes being consistently up- or down-regulated in OVX microglia compared with controls (Fig. 3B). Gene Ontology (GO) enrichment analysis across the three categories (biological process, cellular component, and molecular function) showed that the differentially expressed genes were significantly

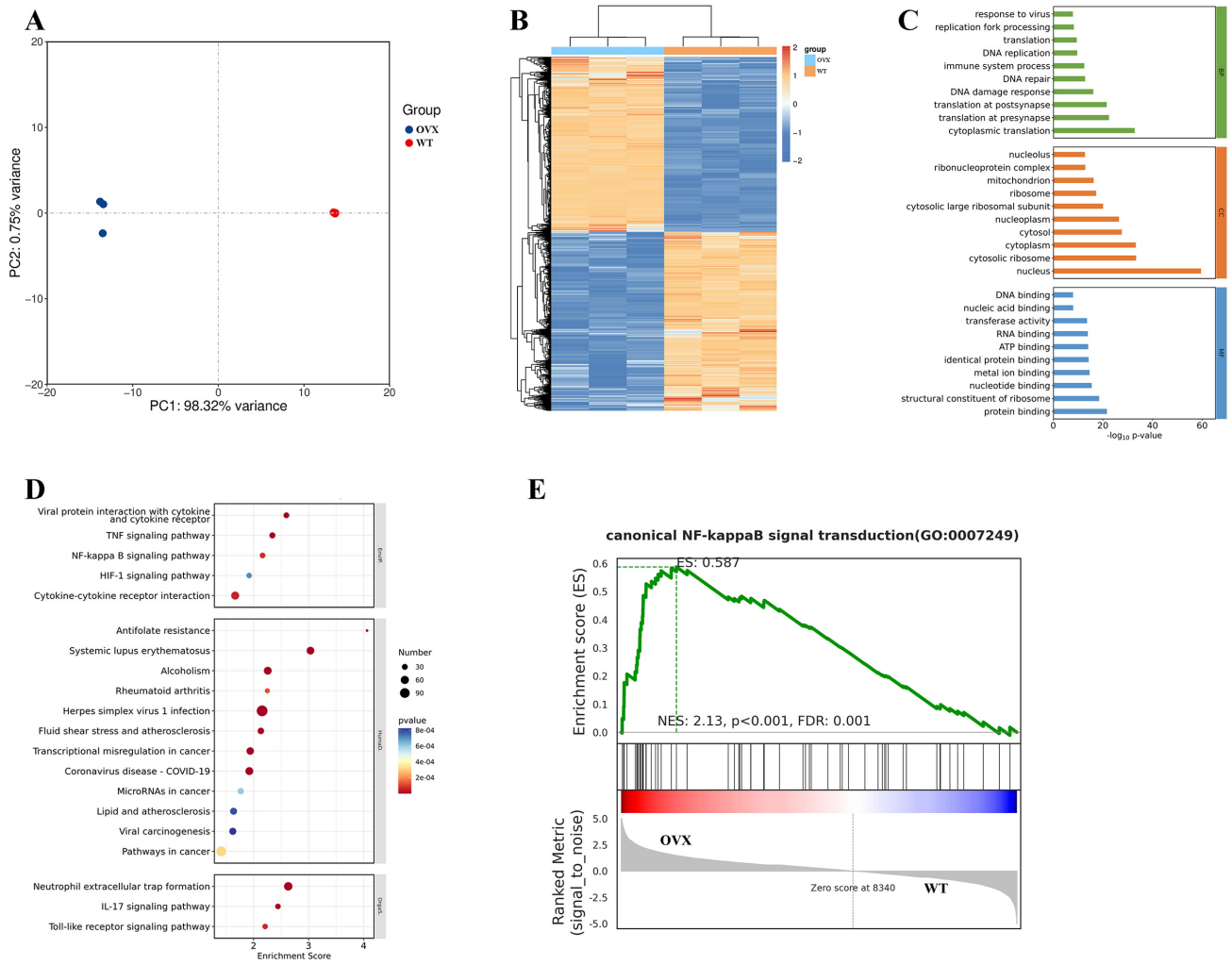


Fig. 3. Transcriptomic analysis of primary microglia from OVX and WT mice (n = 3). (A) PCA analysis. (B) Heatmap analysis of differentially expressed genes. (C) GO enrichment analysis for BP, CC, and MF. (D) KEGG pathway analysis. (E) GSEA for NF-κB pathway. WT, wild-type; PCA, principal component analysis; GO, Gene Ontology; BP, biological process; CC, cellular component; MF, molecular function; NES, normalized enrichment score; FDR, false discovery rate; KEGG, Kyoto Encyclopedia of Genes and Genomes; GSEA, Gene Set Enrichment Analysis; NF-κB, nuclear factor kappa-light-chain-enhancer of activated B cells; ES, enrichment score.

associated with immune response, inflammatory signaling, and metabolic regulation (Fig. 3C). KEGG pathway analysis identified multiple inflammation-related pathways that were altered by OVX, including the canonical NF-κB signaling pathway, the TNF signaling pathway, and the IL-17 signaling pathway (Fig. 3D). Consistent with these findings, GSEA indicated that the NF-κB signaling pathway was significantly activated in OVX microglia compared with WT controls (Fig. 3E). Collectively, these transcriptomic data suggest that ovariectomy drives a coordinated pro-inflammatory and metabolically shifted phenotype in microglia.

3.4 Estradiol Alleviates OVX-Induced Microglial Inflammation

To further characterize microglial status, we qualitatively assessed Iba1$^+$ cell morphology in the hippocampal CA3 region (Fig. 4A). In the representative Control images, Iba1$^+$ cells exhibited a ramified morphology, characterized by a small cell body and fine, extensively branched processes. The representative OVX images showed activated morphological features, including enlarged cell bodies and retracted processes. Sequencing data indicated that OVX led to significant changes in inflammatory signaling within microglia. Immunofluorescence staining (Fig. 4A) confirmed that OVX promoted pro-inflammatory M1 polarization of microglia ($p < 0.001$, Fig. 4B), while E2 treatment attenuated M1 polarization in a concentration-dependent manner (Low: $p = 0.022$; High: $p = 0.006$; Fig. 4B). Furthermore, E2 treatment significantly reduced OVX-induced release of the pro-inflammatory cytokines TNF-α (Low: $p = 0.008$; High: $p < 0.001$; Fig. 4C), IL-1β (Low: $p = 0.004$; High: $p < 0.001$; Fig. 4C) and IL-6 (Low: $p = 0.031$; High: $p < 0.001$; Fig. 4C). Western

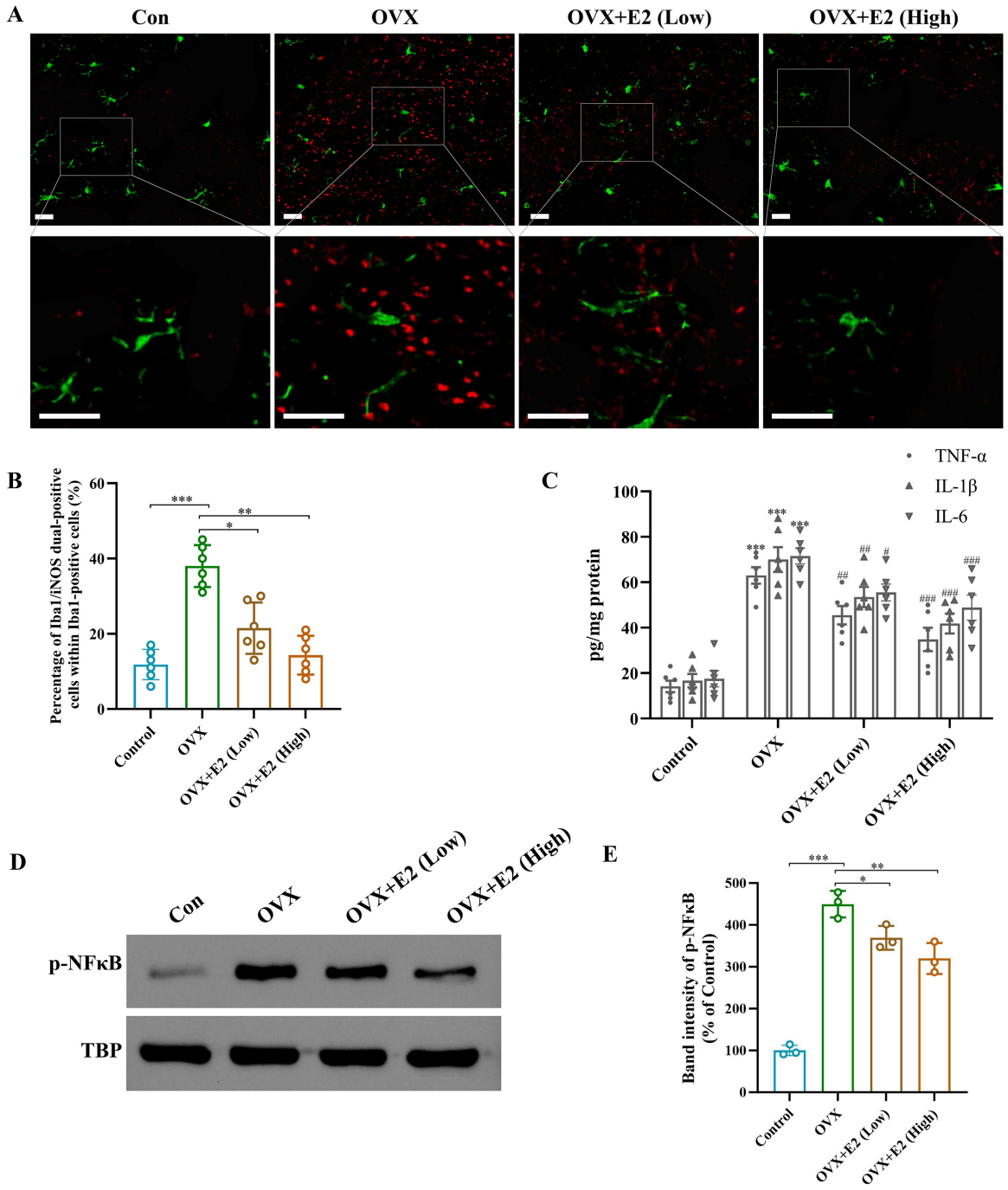


Fig. 4. Effects of OVX and estradiol treatment on microglial inflammation. (A) Representative immunofluorescence images showing microglial M1 polarization markers in the hippocampus. Green fluorescence indicates microglia, and red fluorescence indicates iNOS. Scale bar = 20 μm. (B) Quantitative analysis of M1-polarized microglia, expressed as a percentage of total microglia (n = 6). (C) Levels of pro-inflammatory cytokines TNF-α, IL-1β, and IL-6 in primary microglia (n = 6). (D) Western blot analysis of nuclear phospho-NF-κB p65 (Ser468) abundance in primary microglia. Nuclear phospho-NF-κB p65 (Ser468) abundance was normalized to TATA-binding protein. (E) Bar graph depicting band intensities of nuclear phospho-NF-κB p65 (Ser468) (n = 3). $^{*}p < 0.05$, $^{**}p < 0.01$, $^{***}p < 0.001$. $^{\#}p < 0.05$, $^{\#\#}p < 0.01$, $^{\#\#\#}p < 0.001$ compared to the OVX group. M1, M1 phenotype; iNOS, inducible nitric oxide synthase; TNF-α, tumor necrosis factor-alpha; IL-1β, interleukin-1 beta; IL-6, interleukin-6; TBP, TATA-binding protein.

blot analysis (Fig. 4D, the original Western blot images are available in the **Supplementary Material-WB**) showed that, compared to the Control group, OVX significantly increased nuclear phospho-NF-κB p65 (Ser468) abundance, which was markedly suppressed by E2 treatment (Low: $p = 0.031$; High: $p = 0.005$; Fig. 4D,E). These results suggest

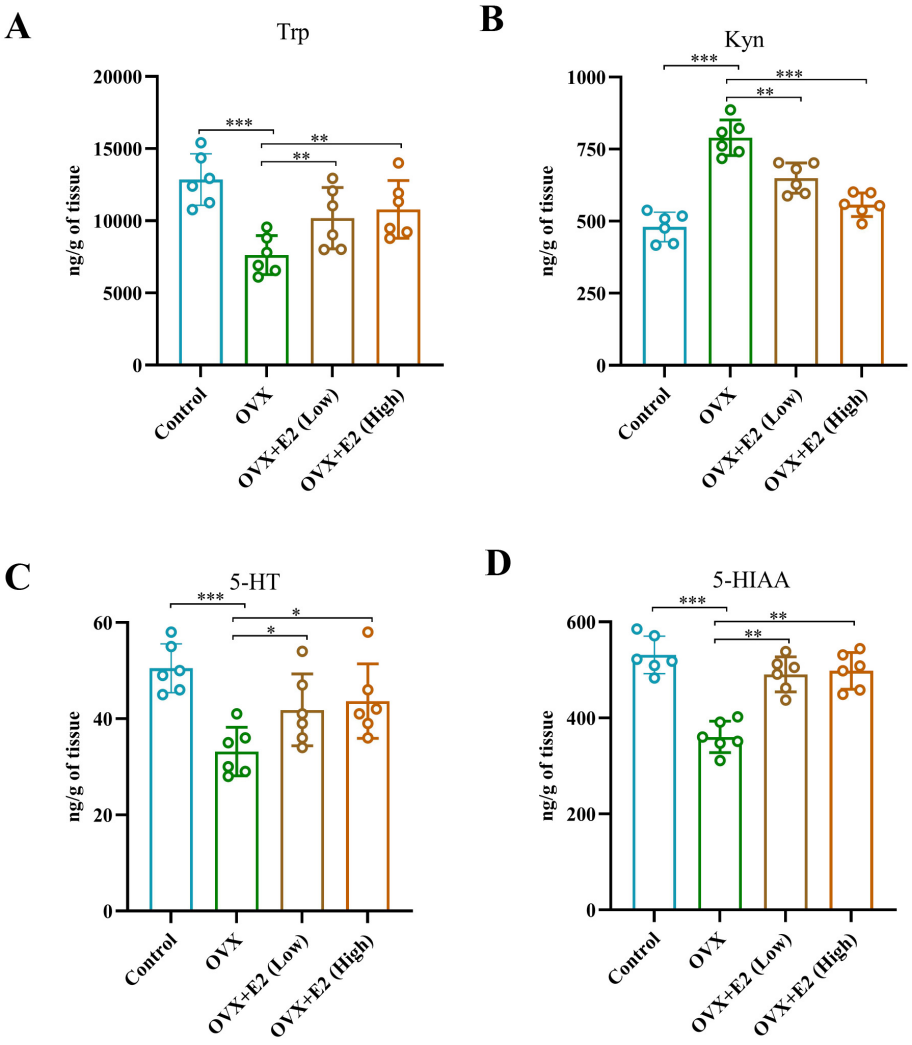


Fig. 5. Effects of OVX and E2 treatment on tryptophan (Trp) and kynurenine (Kyn) levels in primary microglia (n = 6). (A) Trp levels. (B) Abundance of Kyn levels. (C) Abundance of 5-HT levels. (D) Abundance of 5-HIAA levels. *$p < 0.05$, **$p < 0.01$, ***$p < 0.001$. 5-HIAA, 5-hydroxyindoleacetic acid; 5-HT, serotonin.

that OVX promotes inflammatory signaling in microglia, whereas E2 treatment significantly improves the microglial inflammatory microenvironment.

3.5 Effects of Ovariectomy and Estradiol Treatment on Hippocampal Microglial Tryptophan, Kynurenine, and Monoamine Levels

Further, the levels of Trp, Kyn, and monoamine neurotransmitters were measured by ELISA in the hippocampal microglia of each group. Compared to the Control group, the OVX group exhibited a significant decrease in hippocampal Trp levels ($p < 0.001$, Fig. 5A). Conversely, E2 treatment promoted Trp levels in a concentration-dependent manner (Low: $p = 0.008$; High: $p = 0.003$; Fig. 5A). The OVX group also showed significant increase in Kyn levels ($p < 0.001$, Fig. 5B), an effect that was dose-dependently reversed by E2 (Low: $p = 0.007$; High: $p < 0.001$; Fig. 5B). Additionally, the levels of the monoamine neurotransmitter 5-HT ($p < 0.001$, Fig. 5C) and its metabolite 5-hydroxyindoleacetic acid (5-HIAA, $p < 0.001$, Fig. 5D) were significantly reduced in the OVX group, while E2 administration concentration-dependently elevated both 5-HT (Low: $p = 0.033$; High: $p = 0.021$; Fig. 5C) and 5-HIAA levels (Low: $p = 0.007$; High: $p = 0.005$; Fig. 5D). These data indicate that OVX induces an imbalance in the Trp/Kyn pathway, which is reversed by E2 treatment.

3.6 Estradiol Replacement Reverses Ovariectomy-Induced Dysregulation of Proteins Involved in Tryptophan and Serotonin Metabolism in Microglia

We next examined the expression of proteins involved in tryptophan and serotonin metabolism using primary microglial lysates by Western blot. TPH2 participates in 5-HT synthesis, SERT mediates 5-HT reuptake, and MAO-A participates in 5-HT degradation. IDO1 catalyzes the first step of tryptophan degradation along the kynurenine pathway. Western blot analysis (Fig. 6A) confirmed that E2 replacement significantly suppressed the OVX-induced over-

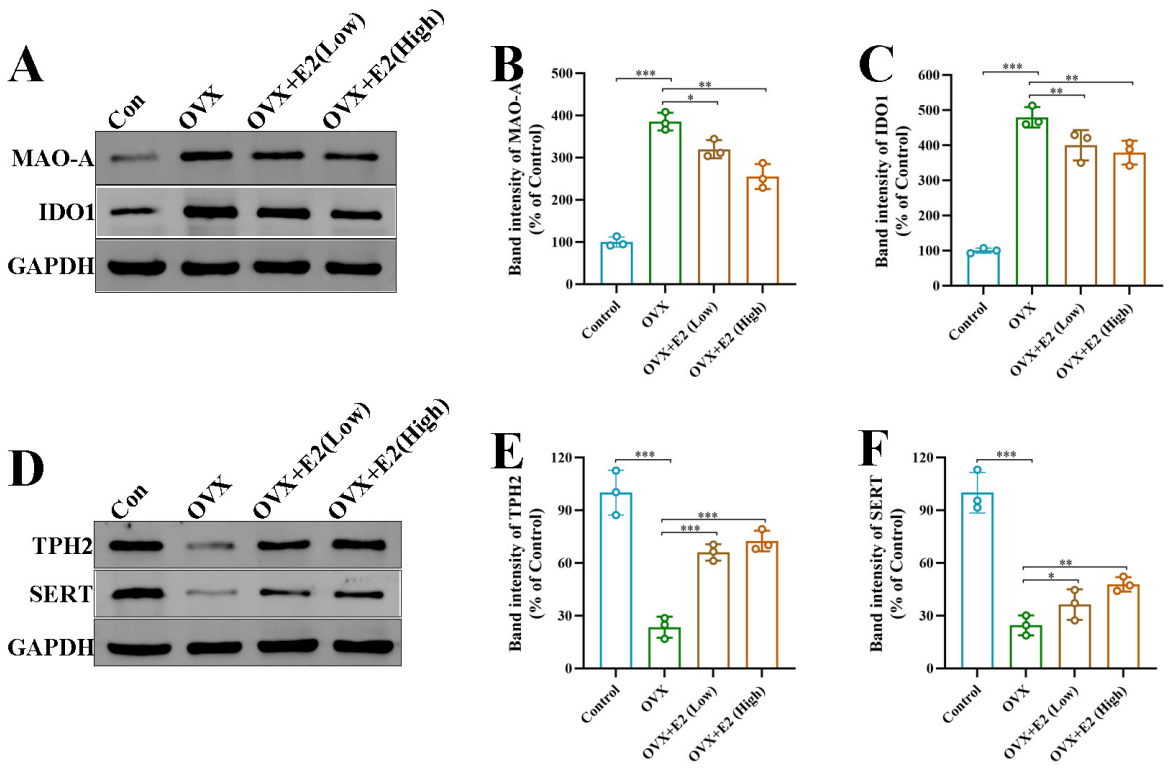


Fig. 6. Estradiol replacement reverses OVX-induced dysregulation of proteins involved in tryptophan and serotonin metabolism in microglia (n = 3). (A) Representative immunoblots showing protein levels of MAO-A and IDO1 in microglia from different treatment groups. (B,C) Densitometric quantification of MAO-A and IDO1. (D) Representative immunoblots showing protein levels of TPH2 and SERT. (E,F) Densitometric quantification of TPH2 and SERT. *$p < 0.05$, **$p < 0.01$, ***$p < 0.001$. MAO-A, monoamine oxidase A; IDO1, indoleamine 2,3-dioxygenase 1; TPH2, tryptophan hydroxylase 2; SERT, serotonin transporter; GAPDH, glyceraldehyde-3-phosphate dehydrogenase.

expression of MAO-A in microglia (Low: $p = 0.027$; High: $p = 0.0038$; Fig. 6B) and IDO1 (Low: $p = 0.006$; High: $p = 0.004$; Fig. 6C). In contrast, E2 markedly reversed the OVX-mediated under expression of TPH2 in microglia (Low: $p < 0.001$; High: $p < 0.001$; Fig. 6E) and SERT (Low: $p = 0.029$; High: $p = 0.0041$; Fig. 6D,F, the original Western blot images are available in the **Supplementary Material-WB**). These data indicate that OVX leads to aberrant expression of proteins involved in tryptophan and serotonin metabolism and that E2 treatment significantly reverses this effect.

4. Discussion

This study describes a clear sequence of events: the loss of estrogen due to ovariectomy triggers two related problems in the hippocampus: microglia-mediated inflammation and disruptions in Trp metabolism. Collectively, these alterations lead to depressive-like behaviors. The reintroduction of E2 reversed all these effects in a dose-dependent manner. This not only confirms the essential role of estrogen in mood regulation but also introduces a novel perspective on postmenopausal depression, not merely conceptualizing it as hormone deficiency but as a condition where the immune system and metabolic processes cease to function synergistically. Such a conceptual paradigm shift matters because it implies that therapeutic strategies should extend beyond hormone replacement therapy, particularly toward interventions that directly address the underlying biological process.

The results reported here add to the existing body of knowledge regarding the relationship between inflammation and depression. Numerous studies have shown that depression is associated with heightened inflammatory signaling and microglial activation, typically in response to stress or in genetic models [21,22]. In this study, removing a single factor (estrogen) was sufficient to induce these processes in the hippocampus. This finding directly links a well-characterized physiological condition (low estrogen levels) to a specific, reproducible immune alteration in the brain [23,24]. This hypothesis is further supported by evidence that anti-inflammatory drugs, such as minocycline, can ameliorate depressive-like behavior in both animal models and preliminary human trials, reinforcing the proposed roles of glial cells in mood disorders [25,26].

The novelty of this investigation lies in examining downstream events triggered by estrogen loss that drive inflammation. Previous studies have linked Kyn pathway dysfunction to depression; these studies have primarily fo-

cused on inflammation elsewhere in the body or on changes in individual enzymes [27,28,29]. In this study, the entire system was analyzed, revealing a coordinated pattern. Following estrogen deficiency, TPH2 and SERT protein levels decrease, whereas MAO-A and IDO1 protein levels increase. This suggests that inflammation actively reroutes Trp utilization rather than merely causing depletion of 5-HT or altering a single enzyme. Importantly, while it is established that inflammation can upregulate IDO1, the data presented herein indicate that concurrently, the brain's capacity to produce 5-HT is also suppressed. These dual effects likely result in reduced availability of 5-HT where it is most needed, while simultaneously facilitating the accumulation of neurotoxic kynurenine metabolites.

Collectively, these immune and metabolic alterations create a cycle that may help explain human depression. Estrogen loss disrupts normal balance, activates microglia, and shifts Trp metabolism toward pathways that produce toxic byproducts, such as quinolinic acid and 3-hydroxykynurenine, which may, in turn, stress neurons and maintain microglial activation [30,31]. Breaking this cycle may offer a viable treatment strategy, particularly for individuals with treatment-resistant depression, who often show signs of low-level inflammation [32,33]. The results reported here suggest that E2 helps not only by acting through classic hormone receptor signaling but also by modulating microglial activity and restoring normal enzyme balance in the Trp-Kyn pathway.

From a clinical perspective, these findings support a framework for understanding depression in the context of menopause. They provide a rationale for considering hormone therapy not solely for the management of symptoms such as hot flashes, but as an early intervention to prevent or mitigate depressive symptoms in perimenopausal and early postmenopausal women, particularly those exhibiting evidence of increased inflammation. For women who are unable to take estrogen, alternative options include drugs that modulate microglial activity, IDO1 inhibitors that cross the blood-brain barrier, or safe MAO-A level modulators. Additionally, the protein expression profile characterized by reduced TPH2 and SERT levels alongside elevated IDO1 and MAO-A could serve as a biomarker for an inflammatory-metabolic subtype of depression, thereby enabling more precise, biologically informed treatment strategies.

Limitations

Nevertheless, some limitations should be noted. The data demonstrate strong correlations and clear dose-response effects, but demonstrating causal relationships requires further study, for example, using cell-specific gene knockouts (such as removing IDO1 only in microglia) or locally blocking these pathways in OVX models. Furthermore, these findings require confirmation in humans, ideally through studies that combine brain imaging of inflammation (e.g., translocator protein positron emission tomography [TSPO-PET]), measurements of Trp metabolites in blood or spinal fluid, and enzyme levels in tissue from depressed postmenopausal women. Although our transcriptomic, ELISA, and Western blot data were all obtained from isolated primary microglia, providing cell-specific evidence, we cannot rule out the possibility that other cell types (e.g., neurons or astrocytes) may also contribute to the observed hippocampal phenotype *in vivo*. The process of microglial isolation inevitably removes them from their native multicellular environment, and paracrine interactions with other cells are lost. Future studies using *in situ* techniques such as single-cell RNA sequencing or spatial transcriptomics would help delineate the relative contributions of different cell types. Finally, while our *in vivo* findings are robust, we did not perform direct *in vitro* studies to confirm the cell-autonomous effects of estradiol on microglia. Given the well-established role of estrogen in brain function, future studies employing primary microglial cultures or BV-2 cells treated with E2 are warranted to provide more precise mechanistic insights. We intend to address this limitation in future research.

5. Conclusions

In summary, this study demonstrates how estrogen loss contributes to depression. It activates microglia in the hippocampus and shifts Trp metabolism toward pathways that produce neurotoxic byproducts. These findings help extend the current understanding of postmenopausal depression beyond a simple state of hormone deficiency, suggesting instead that it may arise from dysregulated crosstalk among the endocrine, immune, and metabolic systems. By integrating these traditionally distinct areas, the present study identifies novel therapeutic targets and potential biomarkers for postmenopausal depression. Furthermore, it supports the development of more personalized biologically informed strategies for depression associated with aging, menopause, and other conditions characterized by chronic estrogen deficiency.

Availability of Data and Materials

Data are available from the corresponding authors upon reasonable request.

Author Contributions

HZ, FX, YX, ZY, YY, LJ and CW conceptualized the study. HZ and LJ carried out the research and performed the experiments. LJ was responsible for data analysis. All authors contributed to editorial changes in the manuscript. All authors have reviewed and approved the final version. All authors have participated sufficiently in the work and agreed to be accountable for all aspects of the work.

Ethics Approval and Consent to Participate

This study was approved by the Institutional Review Board of The Affiliated Nanhua Hospital (2026-ky-046) and was conducted in strict compliance with the National Institutes of Health Guide for the Care and Use of Laboratory Animals and ARRIVE 2.0 (see **Supplementary Material**).

Acknowledgment

We thank YODA Editing for the preparation of the manuscript.

Funding

This work was supported by the Natural Science Foundation of Hunan province (2025JJ90140), Health research project by the Health Commission of Hunan Province (B202303079075) and Hengyang City Science and Technology Innovation Project (202550037866).

Conflicts of Interest

The authors declare no conflicts of interest.

Supplementary Material

Supplementary material associated with this article can be found, in the online version, at https://doi.org/10.31083/JIN52110.

References

[1] Badawy Y, Spector A, Li Z, Desai R. The risk of depression in the menopausal stages: A systematic review and meta-analysis. Journal of Affective Disorders. 2024; 357: 126–133. https://doi.org/10.1016/j.jad.2024.04.041

[2] Pan M, Pan X, Zhou J, Wang J, Qi Q, Wang L. Update on hormone therapy for the management of postmenopausal women. Bioscience Trends. 2022; 16: 46–57. https://doi.org/10.5582/bst.2021.01418

[3] Zuhlsdorff K, Langley C, Bethlehem R, Warrier V, Romero Garcia R, Sahakian BJ. Emotional and cognitive effects of menopause and hormone replacement therapy. Psychological Medicine. 2026; 56: e24. https://doi.org/10.1017/S0033291725102845

[4] Cao Y, Zhao Y, Deng T, Zhou Q, Hu G, Hu ZL, et al. Hepatic acetyl-CoA metabolism modulates neuroinflammation and depression susceptibility via acetate. Cell Metabolism. 2025; 37: 2185–2201.e8. https://doi.org/10.1016/j.cmet.2025.08.010

[5] Wang A, Wan X, Zhuang P, Jia W, Ao Y, Liu X, et al. High fried food consumption impacts anxiety and depression due to lipid metabolism disturbance and neuroinflammation. Proceedings of the National Academy of Sciences of the United States of America. 2023; 120: e2221097120. https://doi.org/10.1073/pnas.2221097120

[6] Woodburn SC, Bollinger JL, Wohleb ES. The semantics of microglia activation: neuroinflammation, homeostasis, and stress. Journal of Neuroinflammation. 2021; 18: 258. https://doi.org/10.1186/s12974-021-02309-6

[7] Xie Y, Chen L, Chen J, Luo Y, Peng Z, Zhang H, et al. Metabotropic Glutamate Receptor 8 Suppresses M1 Polarization in Microglia by Alleviating Endoplasmic Reticulum Stress and Mitochondrial Dysfunction. Journal of Integrative Neuroscience. 2024; 23: 26. https://doi.org/10.31083/j.jin2302026

[8] Picard K, Bisht K, Poggini S, Garofalo S, Golia MT, Basilico B, et al. Microglial-glucocorticoid receptor depletion alters the response of hippocampal microglia and neurons in a chronic unpredictable mild stress paradigm in female mice. Brain, Behavior, and Immunity. 2021; 97: 423–439. https://doi.org/10.1016/j.bbi.2021.07.022

[9] Mokhtari T, Irandoost E, Sheikhbahaei F. Stress, pain, anxiety, and depression in endometriosis-Targeting glial activation and inflammation. International Immunopharmacology. 2024; 132: 111942. https://doi.org/10.1016/j.intimp.2024.111942

[10] Xue C, Li G, Zheng Q, Gu X, Shi Q, Su Y, et al. Tryptophan metabolism in health and disease. Cell Metabolism. 2023; 35: 1304–1326. https://doi.org/10.1016/j.cmet.2023.06.004

[11] Ramprasath T, Han YM, Zhang D, Yu CJ, Zou MH. Tryptophan Catabolism and Inflammation: A Novel Therapeutic Target For Aortic Diseases. Frontiers in Immunology. 2021; 12: 731701. https://doi.org/10.3389/fimmu.2021.731701

[12] Salminen A. Role of indoleamine 2,3-dioxygenase 1 (IDO1) and kynurenine pathway in the regulation of the aging process. Ageing Research Reviews. 2022; 75: 101573. https://doi.org/10.1016/j.arr.2022.101573

[13] Ge PY, Qu SY, Ni SJ, Yao ZY, Qi YY, Zhao X, et al. Berberine ameliorates depression-like behavior in CUMS mice by activating TPH1 and inhibiting IDO1-associated with tryptophan metabolism. Phytotherapy Research: PTR. 2023; 37: 342–357. https://doi.org/10.1002/ptr.7616

[14] Luengo-Mateos M, González-Vila A, Torres Caldas AM, Alasaoufi AM, González-Domínguez M, López M, et al. Protocol for ovariectomy and estradiol replacement in mice. STAR Protocols. 2024; 5: 102910. https://doi.org/10.1016/j.xpro.2024.102910

[15] Liu MY, Yin CY, Zhu LJ, Zhu XH, Xu C, Luo CX, et al. Sucrose preference test for measurement of stress-induced anhedonia in mice. Nature Protocols. 2018; 13: 1686–1698. https://doi.org/10.1038/s41596-018-0011-z

[16] Steru L, Chermat R, Thierry B, Simon P. The tail suspension test: a new method for screening antidepressants in mice. Psychopharmacology. 1985; 85: 367–370. https://doi.org/10.1007/BF00428203

[17] Porsolt RD, Bertin A, Blavet N, Deniel M, Jalfre M. Immobility induced by forced swimming in rats: effects of agents which modify central catecholamine and serotonin activity. European Journal of Pharmacology. 1979; 57: 201–210. https://doi.org/10.1016/0014-2999(79)90366-2

[18] Walsh RN, Cummins RA. The Open-Field Test: a critical review. Psychological Bulletin. 1976; 83: 482–504. https://doi.org/10.1037/0033-2909.83.3.482

[19] Nikodemova M, Watters JJ. Efficient isolation of live microglia with preserved phenotypes from adult mouse brain. Journal of Neuroinflammation. 2012; 9: 147. https://doi.org/10.1186/1742-2094-9-147

[20] Lee JK, Tansey MG. Microglia isolation from adult mouse brain. Methods in Molecular Biology (Clifton, N.J.). 2013; 1041: 17–23. https://doi.org/10.1007/978-1-62703-520-0_3

[21] Song J, Kim YK. Animal models for the study of depressive disorder. CNS Neuroscience & Therapeutics. 2021; 27: 633–642. https://doi.org/10.1111/cns.13622

[22] Zhang Y, Wu S, Tang W, Yang C, Yin Y, He J, et al. The Role of the Hippocampal P2X7R/NLRP3 Signaling Pathway in Depression-Like Behavior Induced by the Interaction Between Chronic Stress and Time in a Rat Model of Stroke. Journal of integrative neuroscience. 2025; 24: 40005. https://doi.org/10.31083/JIN40005

[23] Shepherd R, Cheung AS, Pang K, Saffery R, Novakovic B. Sexual Dimorphism in Innate Immunity: The Role of Sex Hormones and Epigenetics. Frontiers in Immunology. 2021; 11: 604000. https://doi.org/10.3389/fimmu.2020.604000

[24] Debs SR, Conn I, Navaneethan B, Penklis AG, Meyer U, Killcross S, et al. Maternal immune activation and estrogen receptor modulation induce sex-specific dopamine-related behavioural and molecular alterations in adult rat offspring. Brain, Behavior, and Immunity. 2024; 118: 236–251. https://doi.org/10.1016/j.bbi.2024.02.034

[25] Hellmann-Regen J, Clemens V, Grözinger M, Kornhuber J, Reif A, Prvulovic D, et al. Effect of Minocycline on Depressive Symptoms in Patients With Treatment-Resistant Depression: A Randomized Clinical Trial. JAMA Network Open. 2022; 5: e2230367. https://doi.org/10.1001/jamanetworkopen.2022.30367

[26] Sakurai M, Iwasa R, Sakai Y, Morimoto M. Minocycline prevents depression-like behavior in streptozotocin-induced diabetic mice. Neuropathology: Official Journal of the Japanese Society of Neuropathology. 2021; 41: 109–117. https://doi.org/10.1111/neup.12706

[27] Lin Y, Wang L, Meng S, Liu J, Li X, Wang W, et al. 3-hydroxykynurenine increase in kynurenine pathway driven bisphenol F induced anxiety- and depression-like behaviors. The Science of the Total Environment. 2025; 995: 180073. https://doi.org/10.1016/j.scitotenv.2025.180073

[28] Cheng J, Gao Y, Liu P, Zhang J, Zhou J. Paeoniflorin attenuates neuropathic Pain-associated depression by modulating microglial M1 polarization and correcting kynurenine pathway dysregulation. International Immunopharmacology. 2025; 164: 115351. https://doi.org/10.1016/j.intimp.2025.115351

[29] Wu X, Chen B, Di Z, Jiang S, Xu H, Shi M, et al. Involvement of kynurenine pathway between inflammation and glutamate in the underlying etiopathology of CUMS-induced depression mouse model. BMC Neuroscience. 2022; 23: 62. https://doi.org/10.1186/s12868-022-00746-4

[30] Dongol A, Chen X, Zheng P, Seyhan ZB, Huang XF. Quinolinic acid impairs mitophagy promoting microglia senescence and poor healthspan in C. elegans: a mechanism of impaired aging process. Biology Direct. 2023; 18: 86. https://doi.org/10.1186/s13062-023-00445-y

[31] Tao X, Yan M, Wang L, Zhou Y, Wang Z, Xia T, et al. Homeostasis Imbalance of Microglia and Astrocytes Leads to Alteration in the Metabolites of the Kynurenine Pathway in LPS-Induced Depressive-Like Mice. International Journal of Molecular Sciences. 2020; 21: 1460. https://doi.org/10.3390/ijms21041460

[32] Nettis MA, Lombardo G, Hastings C, Zajkowska Z, Mariani N, Nikkheslat N, et al. Augmentation therapy with minocycline in treatment-resistant depression patients with low-grade peripheral inflammation: results from a double-blind randomised clinical trial. Neuropsychopharmacology: Official Publication of the American College of Neuropsychopharmacology. 2021; 46: 939–948. https://doi.org/10.1038/s41386-020-00948-6

[33] Chen MH, Su TP, Lin WC, Li CT, Wu HJ, Tsai SJ, et al. Rapid Antidepressant and Antisuicidal Effects of Low-Dose Ketamine Infusion in Patients With Treatment-Resistant Depression With or Without Low-Grade Inflammation. Pharmacopsychiatry. 2025; 58: 235–241. https://doi.org/10.1055/a-2499-7207